# Fusion Boundary Cracking in CuNi10Fe Alloy Weldments

Reprinted from
*Joining Sciences*
Volume 1, Number 1, April 1991

NiDI
NICKEL DEVELOPMENT INSTITUTE
NiDI Reprint Series No 14 016

**Dr. Norman Stephenson**

# Fusion Boundary Cracking in CuNi10Fe Alloy Weldments

By N. Stephenson*

**Summary**

**Effects of parent material purity, weld heat-input and weld metal composition on fusion boundary cracking when welding thick, wrought, CuNi10Fe alloy plates are illustrated and discussed. Attention is given to the likely role of reactive additions in offsetting the adverse influence of impurity elements.**

## Introduction

The CuNi10Fe alloy (CA706) is used widely in main and ancillary systems handling seawater in ships, on offshore platforms, in desalination plant and in various type of plant at coastal and estuarine sites. Over the past quarter century, many thousands of tonnes of the alloy have been so employed, and service experience has been very satisfactory. Apart from early difficulties, there have been few metallurgical problems in weld fabrication and assembly. Among the initial difficulties was the incidence of weld fusion boundary cracking in material from certain sources, and the defect has recurred occasionally, notably when joining thicker sections and making restrained welds, especially at high weld heat-inputs. Also, the defect has been encountered when welding clad steel plate.

* N. Stephenson, B.Met., Ph.D is a UK consultant to the Nickel Development Institute.

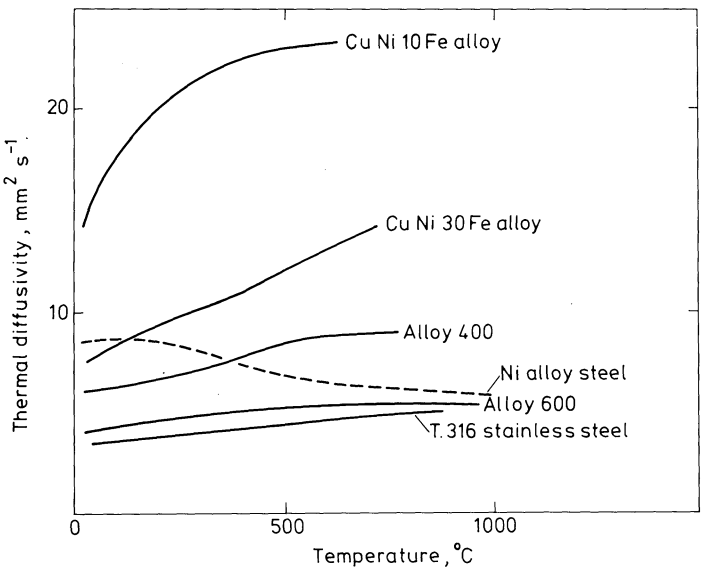


1 Thermal diffusivities of CuNi10Fe alloy compared with those of other materials. (Derived using data from various sources).

Consumables for welding the alloy to itself, and to other cupro-nickels, almost invariably are of the CuNi30 type (ECuNi and ERCuNi), because the somewhat higher melting point is helpful in avoiding lack of fusion faults associated with the high thermal diffusivity of the CuNi10Fe parent material and weld metals (Fig 1). Even so, for corresponding weld geometries and welding processes, the heat-inputs are rather higher than those appropriate to many other materials. There is evidence that the CuNi10Fe weld deposits display unsatisfactory resistance to corrosion by seawater[1]; also, strengths may be inadequate. NiCu30Mn consumables (ENiCu-7 and ERNiCu-7) are used in the welding of clad steels, and the joints may be capped with CuNi30 weld metal.

Cracking in copper-nickel alloy weldments has long been linked with the presence of impurity elements, such as Bi, Te, Pb, Se, S and P, which segregate towards grain boundaries where low melting point eutectics may be formed and/or grain boundary cohesion impaired. 'Liquation' cracking and/or 'ductility dip' cracking may ensue during welding. The literature has recently been reviewed extensively elsewhere.[2] Through the years, systematic investigations and successive improvements in analytical techniques have enabled the relative effects of various subversive elements to be assessed with greater precision.[3,4,5,6,7] It became evident that the presence of even a few parts per million of the more virulent impurities, such as Bi and Te, can be detrimental to both weldability and hot workability. However, in the literature, little attention has been given to the influence of elements whose presence may be beneficial.

The present paper illustrates some effects of parent material purity, weld heat-input and weld metal composition on fusion boundary cracking in weldments involving thick, wrought, CuNi10Fe plates. Considerations of productivity directed attention mainly towards the behaviour of high heat-input welds. The probable role of so-called 'finishing additions' in offsetting the adverse effects of impurity elements is discussed.

## Materials, Procedure and Results of Welding Trials

The observations were made during an investigation aimed primarily at the elimination of strong arc-deflection encountered when joining thick CuNi10Fe to CuNi30Fe alloy plates by the SMAW process with flux-coated CuNi30 and NiCu30 electrodes, no other process being acceptable for the fabrication concerned. Arc-deflection was towards the CuNi30Fe material. A solution to that problem was obtained by using a commercially-available, electronically-controlled, power source having an optional square-wave AC

Table I. Compositions of CuNi10Fe alloy plates (copper : balance)

| Element | Plate R1 | R2 | F1 | E1 | S1 |
|---|---|---|---|---|---|
| | Composition, wt. % | | | | |
| Ni | 10.4 | 10.8 | 10.4 | 10.3 | 9.41 |
| Fe | 1.73 | 1.80 | 1.46 | 1.50 | 1.40 |
| Mn | 0.80 | 0.8 | 0.8 | 0.76 | 0.63 |
| Si | <0.01 | <0.01 | <0.01 | 0.015 | <0.01 |
| C | 0.002 | 0.0017 | 0.0050 | 0.001 | 0.005 |
| Mg | n.a. | <0.005 | 0.005-0.01 | <0.005 | <0.005 |
| Ca | n.a. | <0.001 | <0.001 | n.a. | n.a. |
| B | <0.002 | <0.002 | <0.001 | n.a. | n.a. |
| Li | <0.001 | <0.001 | <0.001 | n.a. | n.a. |
| Ti | <0.01 | <0.01 | <0.01 | n.a. | n.a. |
| Zr | <0.01 | <0.01 | <0.01 | n.a. | n.a. |
| | Impurities, ppm | | | | |
| O (total) | 25 | 25 | 12 | 55 | 15 |
| P | <20 | <20 | <20 | <20 | <20 |
| As* | 131 | 83 | 16 | 7 | 13 |
| S | 95 | 95 | 30 | 45 | 20 |
| Se* | <1 | 22 | 31 | <1 | <1 |
| Pb* | 46 | 35 | 13 | 12 | 4 |
| Te* | <1 | 6 | <1 | <1 | <1 |
| Bi* | 2 | 2 | 2 | <1 | <1 |
| Zn | 1000 | 700 | 100 | <100 | ca. 100 |
| Sn | ca. 50 | 20-50 | <20 | <50 | <50 |
| Sb | <50 | <50 | <50 | <50 | <50 |
| Cd | <10 | <10 | <10 | <10 | <10 |
| Al | <50 | <50 | <50 | <50 | <50 |
| Ag | ca. 100 | 20-50 | 20-50 | <10 | ca. 50 |

n.a. = not analysed * atomic absorption technique

output which could be biased to alter the relative durations of the positive and negative parts of the AC cycle.[8] Recovery during voltage-reversal in the AC cycle was so rapid that the electrodes, normally recommended for DC+ operation only, could readily be run AC. Arc-strike voltages were DC and acceptably safe. When joining thick plates, the arc-deflection could not always be overcome completely at appropriate welding currents without using the biasing capability in conjunction with enhanced bevel angles.

During the work, fissures were encountered at several of the CuNi10Fe plate/CuNi30 weld metal junctions. The initial arc-deflection difficulties pointed to lack-of-fusion, but metallographic examinations showed that the defects were fusion boundary cracks. Commensurate cracking occurred also in joints, made under comparable conditions, between crack-prone CuNi10Fe plates by conventional electrode DC+technique.

In the trials, 14-16 mm thick CuNi10Fe plates with 55°-60° single-bevels were tee-welded, predominantly with CuNi30 electrodes, to CuNi30Fe plates, 22-28 mm thick. The plates were obtained from a number of sources and had been variously annealed, but the results of side tests indicated that heat-treatment variations, including cooling rate, had little if any influence on fusion boundary cracking and, incidentally, only minor effects on arc-deflection. Owing to progressive closure of the root gaps, difficulties were encountered in securing penetration, despite close tacking. Penetration by higher-melting-point weld metal from a NiCu30Mn electrode was better but remained erratic, and susceptibility to fusion boundary cracking was increased by comparison with that encountered with the CuNi30 electrodes. Reverting to a CuNi30 electrode, root-penetration was obtained by tacking at 50 mm intervals and, where necessary, maintaining the root gap by progressive cutting with a thin flexible saw blade. The welds were assessed by visual inspection, bend tests and microscopical examination of transverse sections.

Crack-free, multi-run, restrained tee-welds were made, without arc-deflection, in the horizontal-vertical (H-V), overhead (O-H) and upward-vertical (U-V) positions, at weld heat-inputs in the ranges 1.1-2.4, 0.9-1.9 and 2.2-4.0kJ/mm, respectively, when the quality of the CuNi10Fe plates was adequate. The electrode was to AWS/SFA — 5.6 ECuNi specification.

The U-V welds experienced higher average heat-inputs, because of the electrode weaving mode which, however, could be adjusted to provide a range of heat-inputs. The poorer quality CuNi10Fe plates suffered severe fusion boundary cracking in H-V and O-H welds and catastrophic cracking in U-V welds. Further tee-welds, notably in the U-V position, were made at various heat-inputs with a view to discriminating between the CuNi10Fe plates. Propensity to fusion boundary cracking increased with heat-input, the finding being contrary to the results of earlier work.[3] There was no practicable minimum heat-input for avoidance of cracks at the fusion boundaries of the worst plates. On the other hand, the best plate withstood U-V runs of more than 12kJ/mm without cracking. No defects were found in the weld heat-affected zones or at the weld fusion boundaries of the CuNi30Fe plates.

Table I gives in detail the compositions of the CuNi10Fe plates all of which conformed readily to the various national specifications. Included is the composition of a sample from a plate, F1, which suffered fusion boundary cracking when welded elsewhere in a U-V configuration similar to that described in this paper; cracking was encountered also in the weld HAZ away from the fusion boundary.

Susceptibility to fusion boundary cracking was in the descending order: R1 = R2, F1, E1, S1.

Welds were made also with a CuNi30 electrode depositing weld metal with iron content ca. 1.4% which is higher than in deposits from electrodes to the AWS/SFA — 5.6 ECuNi specification (ca. 0.6% Fe) including that from the proprietary electrode used to produce the sound joints. Under comparable welding conditions and using crack-prone plates, an appreciable increase of fusion boundary cracking was observed.

Typical all-weld-metal compositions are given in Table II. No weld metal cracking was encountered.

Table II. All-weld metal compositions for flux-coated electrodes (copper : balance)

| Element | Electrode | | |
|---|---|---|---|
| | CuNi30MnFe* | CuNi30FeMn* | NiCu30Mn** |
| | Composition, wt. % | | |
| Ni | 29.3 | 28.9 | 62.0-68.0 |
| Mn | 1.99 | 1.13 | 4.0 max |
| Fe | 0.54 | 1.42 | 2.5 max |
| Si | 0.14 | 0.18 | 1.0 max |
| Ti | 0.17 | 0.23 | 1.0 max |
| C | 0.009 | 0.012 | 0.15 max |
| | Impurities, ppm | | |
| P | 110 | 25 | 200 max |
| As | <100 | <100 | |
| S | 50 | 30 | 150 max |
| Se† | < 1 | < 1 | |
| Pb | <20 | ca. 20 | |
| Te† | < 1 | < 1 | |
| Bi† | < 1 | < 1 | |
| Zn | <100 | <100 | |
| Sn | <100 | ca. 100 | |
| Sb | < 50 | < 50 | |
| Al | ca. 50 | ca. 500 | |
| Ag | 20-50 | 50-100 | |

* : typical composition
** : manufacturer's nominal composition
† : atomic absorption technique

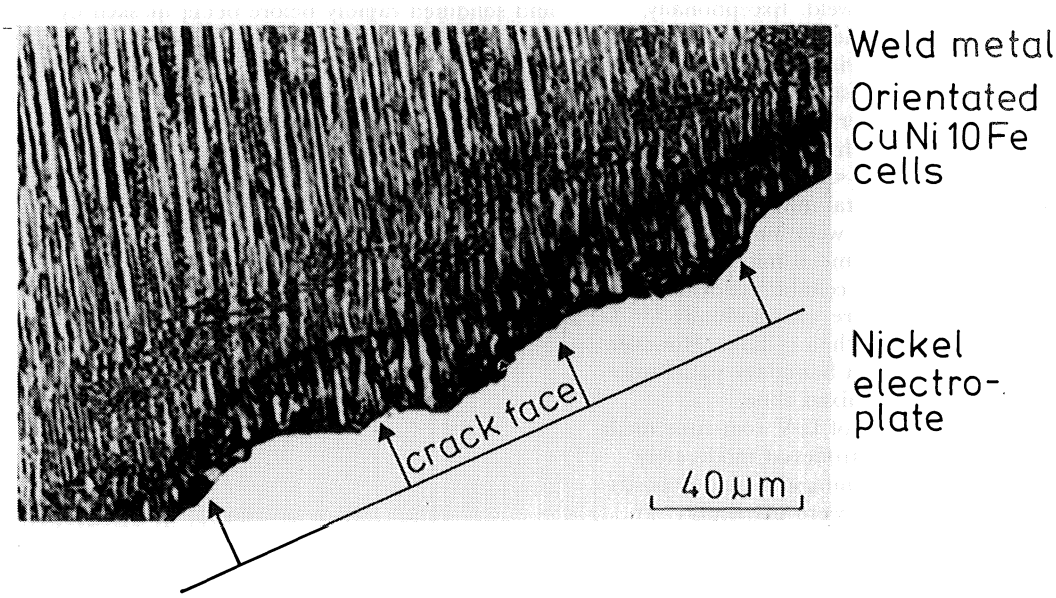


**2** Broken portion (weld metal side) of high heat-input U-V weld made in plate R2 with CuNi30FeMn electrode. Illustration shows orientated CuNi10Fe solidification cells and main location of fusion boundary cracking.

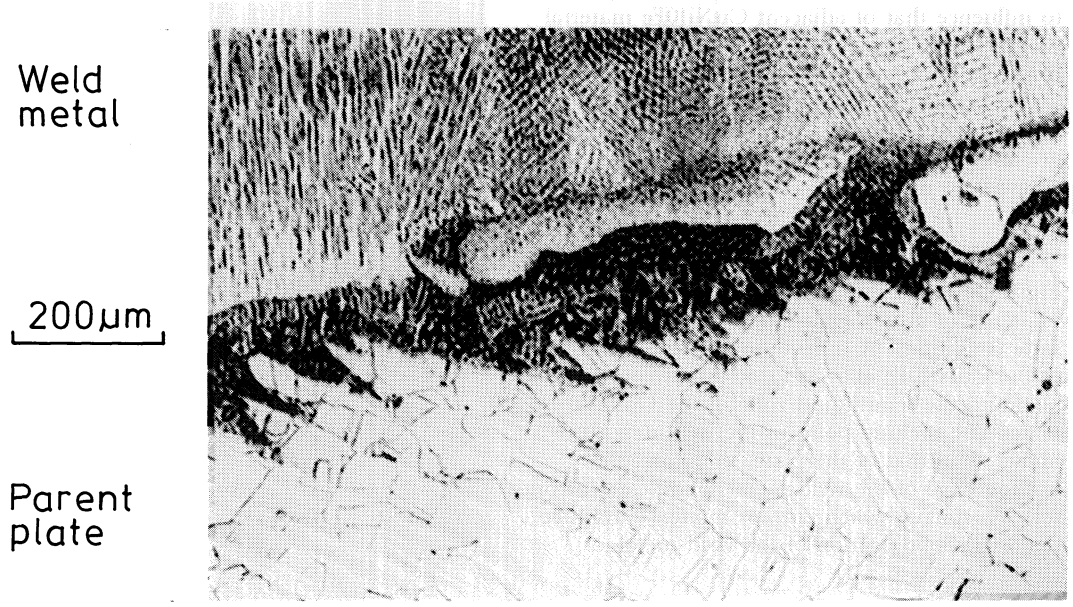


**3** High heat-input U-V weld made in plate R2 with CuNi30MnFe electrode. Illustration shows heterogeneity of weld deposit at fusion boundary.

## Metallography

In the high heat-input (>3kJ/mm) welds, a feature of the solidification pattern was a layer of orientated CuNi10Fe cells adjacent to the CuNi30 weld metal (Fig 2) and, on the microscopical scale, persisting over long lengths of the boundary. Continuity was interrupted by the effects of separate small portions of weld deposit (Fig 3). Next to such portions, cracks were found occasionally at places where molten CuNi10Fe material had been trapped by, or had intruded into the weld deposit (Fig 4). In those regions, as well as along the fusion boundary, the orientations of the regular CuNi10Fe cells were strongly influenced by those of adjacent weld metal cellular dendrites. Towards the CuNi10Fe plate, beyond the layer of orientated CuNi10Fe cells, the microstructure was much more random. The fusion boundary fissuring occurred along a substantially continuous grain boundary which ran mainly along the terminals of the orientated CuNi10Fe cells (Fig 2) but which diverted occasionally into the more disorientated region of the unmixed zone (Fig 5).

Grain boundaries that had been heavily liquated, and 'ghost' grain boundaries resulting from boundary migration after solidification of liquated material, were observed in the parent CuNi10Fe plate near the weld. Exceptionally, gaseous activity in the weld heat-affected zone had driven liquated material into the unmixed fused region (Fig 6). Liquation effects were much less evident with the better CuNi10Fe plates.

In a weld produced with a CuNi30 electrode at relatively low heat-input (<2kJ/mm), there was little evidence of weld metal inhomogeneity or of epitaxial growth from the weld metal into the unmixed zone. The weld metal microstructure was dendritic rather than cellular/dendritic and the unmixed zone structure was randomly granular/dendritic rather than cellular. However, continuous irregular grain boundary paths were discernible along the unmixed zone.

In the transition zones of U-V root-runs made with the NiCu30Mn electrodes at moderately high heat-inputs, ca. 3kJ/mm, the weld deposits near the fusion boundary were markedly heterogeneous, owing to incomplete mixing with the fused CuNi10Fe material (Fig 7). The tendency of the weld metal solidification pattern to influence that of adjacent CuNi10Fe material was apparent only in the heterogeneous regions of the weld deposit somewhat away from the fusion boundary. Cracking was predominantly along the fusion boundary, between randomly-orientated grains of the solidified CuNi10Fe alloy adjacent to the plate.

## Discussion

Fig 8 illustrates the probable solidification sequence of a high heat-input weld under steady state conditions. A thin, unmixed, molten zone of the CuNi10Fe alloy is formed between the weld pool and the semi-liquid zone of the CuNi10Fe plate. The melting point of the weld deposit is higher than that of the plate; therefore, the leading edge of the weld metal solidification front forms a tongue which entraps molten CuNi10Fe material. Solidification of the weld metal continues by cellular dendritic growth towards the weld pool centre.

The tongue may be cracked by weld pool turbulence to admit intrusions of the liquid CuNi10Fe alloy. It may be broken away and partly remelted in a hotter part of the weld pool before the remainder impinges on the unmixed zone and displaces molten CuNi10Fe material. Additionally, weld metal globules may be trapped and solidified rapidly before being masked by weld metal in bulk. Accordingly, there are irregularities at the fusion boundary and the nearby weld metal is heterogeneous. Those effects are more evident in welds made with the NiCu30 rather than the CuNi30 electrodes, because of the greater difference between the melting point of the weld metal and the CuNi10Fe material.

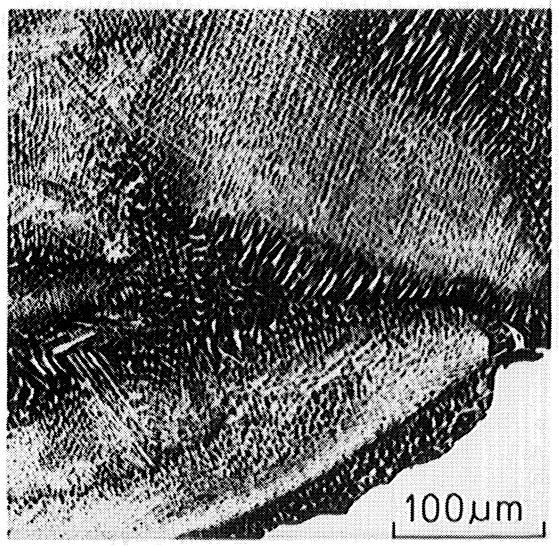


**4** Broken portion (weld metal side) of high heat-input U-V weld made in plate R2 with CuNi30FeMn electrode. Illustration shows fissures in CuNi10Fe intrusions.

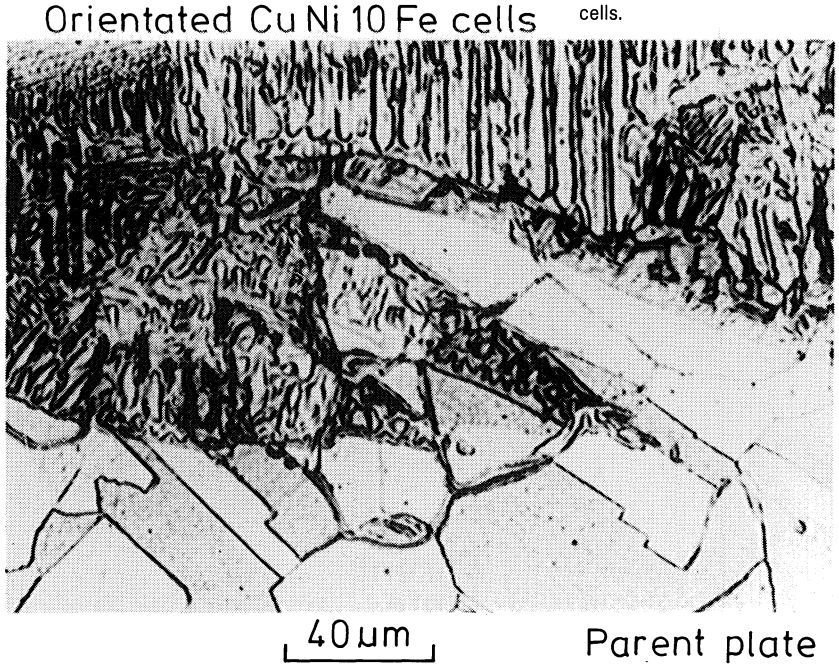


**5** High heat-input U-V weld made in plate R2 with CuNi30FeMn electrode. Illustration shows continuation of grain boundary between disorientated solidification cells.

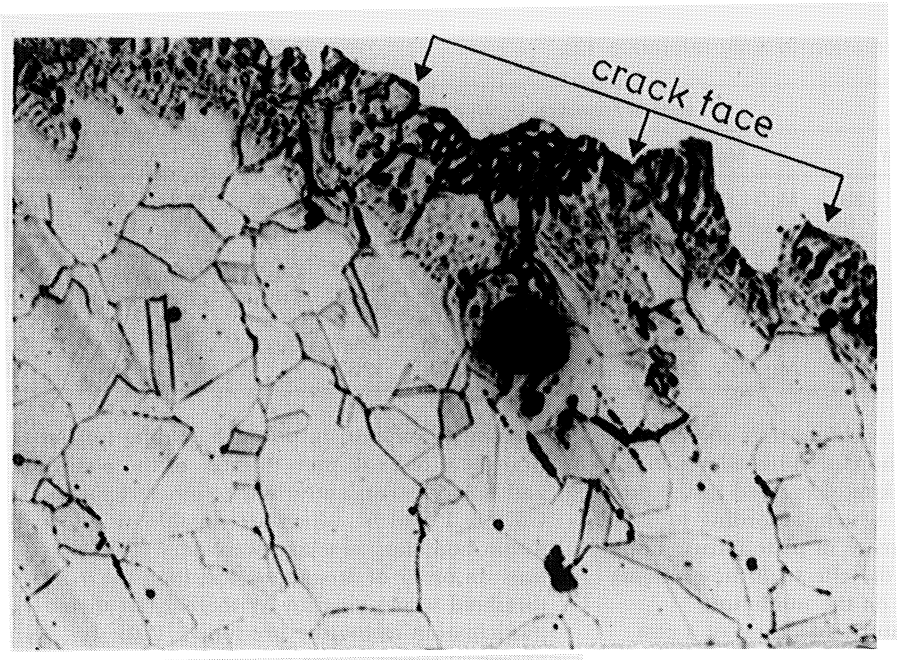


**6** Broken portion (plate side) of high heat-input U-V weld made in plate R2 with CuNi30FeMn electrode. Figure shows extrusion of molten material from gas pore in liquated region of plate.


**7** U-V weld root-run, at ca 3kJ/mm, made in plate S1 with NiCu30Mn electrode. Illustration shows heterogeneity of weld deposit.

On the other side of the weld metal tongue, orientated cells of the CuNi10Fe alloy grow from solidified CuNi30 weld metal into the unmixed CuNi10Fe molten zone, and locally they may become disorientated. The apparently anomalous growth down the weld thermal gradient is feasible because of constitutional supercooling which is encouraged by large weld pools and by the high thermal diffusivity of the CuNi10Fe plate.[9] Epitaxy is favoured also by the overlap or near-coincidence of the CuNi30 weld metal solidus and the CuNi10Fe liquidus and probably by prior superficial diffusion between weld metal and fused unmixed material. On the other hand, the gap between the high-nickel NiCu30Mn weld metal solidus and the CuNi10Fe liquidus discourages continuation of cell growth into the CuNi10Fe liquid.

After peak temperatures are attained in the weld heat-affected zone (HAZ) of the parent plate, solidification proceeds along the liquated grain boundaries towards the unmixed zone until irregular solidification cells and grains can grow. The liquid trapped by the growth of the two CuNi10Fe systems, converging respectively from the directions of the CuNi30 weld metal and the HAZ, becomes progressively richer in copper and impurities and is the last material to solidify in the unmixed region. The interface is a grain boundary which is the preferred site of the fissuring.

In the welds made at low heat-inputs, the thermal conditions are much less favourable to constitutional supercooling[9]. Accordingly, the weld metal solidification patterns are dendritic rather than cellular/dendritic, and randomly-orientated fine grains extend over the unmixed zone. The diminished levels of impurities per unit area of grain boundary, together with the more rapid imposition of thermal stresses during cooling, will improve the hot ductility and decrease the propensity to cracking.

**8** Diagrammatic representation of solidification at weld fusion boundary of high heat-input weld.

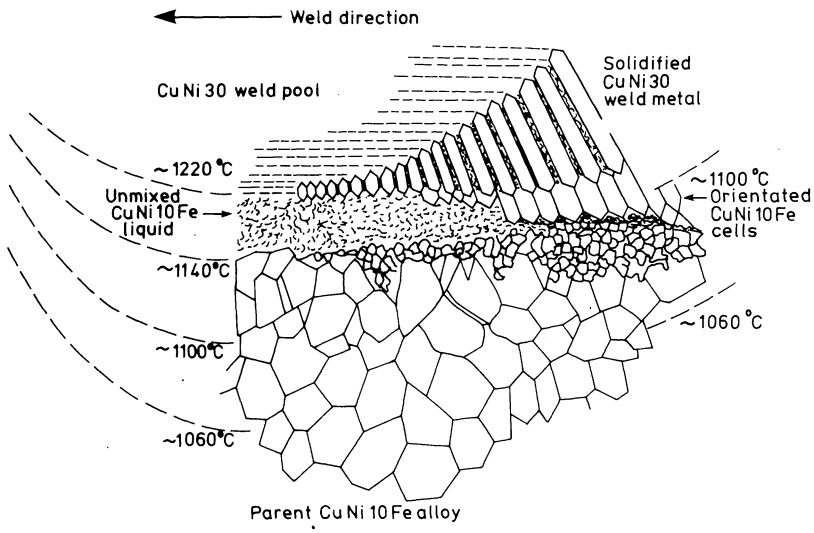

Table III. Heats of Formation (mainly reference 12).

| Impurity element | Heat of Formation ($-\Delta H$) at 20°-25°C, kJ/mol. | | | | | | | | | | | |
|---|---|---|---|---|---|---|---|---|---|---|---|---|
| | Mn | | Mg | | Ca | | Li | | Cu | | Ni | |
| O | MnO | 385 | MgO | 602 | CaO | 634 | $Li_2O$ | 597 | $Cu_2O$ | 168 | NiO | 241 |
| P | MnP | 96 | $Mg_3P_2$ | 465 | $Ca_3P_2$ | 506 | | | $Cu_3P$ | 129 | $Ni_3P$ | 200 |
| As | MnAs | 59 | $Mg_3As_2$ | 373 | | | | | | | | |
| S | MnS | 214 | MgS | 352 | CaS | 476 | $Li_2S$ | 447 | $Cu_2S$ | 80 | $Ni_3S_2$ | 216 |
| Se | MnSe | 155 | MgSe | 273 | CaSe | 368 | $Li_2Se$ | 402 | $Cu_2Se$ | 65 | NiSe | 75 |
| Pb | | | $Mg_2Pb$ | 48 | $Ca_2Pb$ | 216 | $Li_4Pb$ | 176 | | | | |
| Te | MnTe | 111 | MgTe | 209 | CaTe | 272 | $Li_2Te$ | 356 | $Cu_2Te$ | 42 | NiTe | 36 |
| Bi | MnBi | 20 | $Mg_3Bi_2$ | 127 | $Ca_3Bi_2$ | 528 | $Li_3Bi$ | 232 | | | NiBi | 8 |

The findings of the welding tests showed that the susceptibility of the CuNi10Fe alloy plates to fusion boundary cracking decreased in the order R1 = R2, F1, E1, S1 which, according to Table I, is the order of increase in plate purity. From an investigation into the effects of the elements Bi, Te, Pb, Se and S on the minimum intermediate temperature ductilities of a cast, fine-grained, binary CuNi10 alloy, Gavin *et al*[7] derived a bismuth equivalent formula applicable at low dilutions:

$$Bi_E = Bi + 0.7\ Te + 0.4\ Pb + 0.2\ Se + 0.1\ S$$

The bismuth equivalents for the CuNi10Fe alloy plates were as follows:

| | | Plate Designation | | | | |
|---|---|---|---|---|---|---|
| | | R1 | R2 | F1 | E1 | S1 |
| $Bi_E$, ppm | Max | 31 | 34 | 17 | 11 | 6 |
| | Min | 30 | | 16 | 9 | 4 |

and the formula ranks the plates correctly in order of weldability.

Rigorous correlation is not possible. Thus, fusion boundary cracking was assessed qualitatively. Compositions, grain sizes, grain boundary conditions and stress/strain conditions differ from those of the ductility tests. The effects of the impurities on liquation cracking, if present, are not necessarily the same as on ductility dip cracking. Also, variations in melt finishing technique, casting procedure and plate processing may influence welding response.[10]

The presence of iron in the CuNi10Fe alloy is necessary to promote resistance to impingement attack in service. Chubb *et al.*[6] showed that increase of iron content progressively diminishes the minimum intermediate temperature ductility of the cast, fine-grained, binary Cu-10Ni alloy. From their results, increase of iron content from 1.40% (plate S1) to 1.80% (plate R2) would be equivalent to an increase of ca. 3ppm Bi. Iron segregates towards dendrite and cell centres and will contribute to decrease of ductility by matrix strengthening and, perhaps, at higher levels, by promotion of precipitation hardening.[11] The increase of fissuring brought about by using the CuNi30 electrode which deposited weld metal containing ca. 1.4% iron, or by using a NiCu30Mn electrode, may be ascribed in part to enhanced stress concentration associated with the higher hot strengths of the weld metals.

The plates R1 and R2 contained relatively high levels of arsenic. Unpublished work by Ansuini[4] indicates that arsenic has about one fifth the potency of sulphur, in principle adding further $Bi_E$ values of ca. 2 ppm to those of the plates R1 and R2. The concentrations of other elements, B, Cd, Sb, P and Si, which are capable of inducing fusion boundary cracking were very low — at least an order of magnitude less than the threshold values cited by Witherell[3] but their participation cannot be precluded. Little is known about reactions between impurity elements, although Barbery[10] has drawn attention to the probability of Sb-Fe-P and Si-P interactions.

Manganese, present in the CuNi10Fe alloy primarily as deoxidiser and desulphuriser, improves hot workability and weldability. However, unless the alloy is produced from very pure raw materials, the beneficial effects of that element often are inadequate when welding conditions are severe. Historically, producers of various special alloys and steels have made small additions of master alloys containing highly reactive elements, such as lithium, magnesium, calcium or zirconium, mainly to improve the hot workability of their products, and the practice is applicable to the cupro-nickels. The heat from which plate E1 was processed had been treated with magnesium, and analysis of a sample from plate F1 indicated similar treatment, but the melt finishing practices for the other three plates were not known.

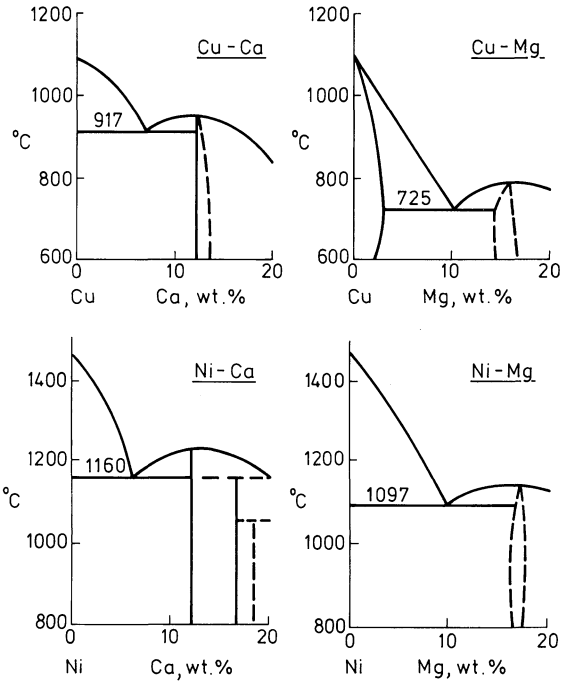


**9** Copper/nickel — calcium/magnesium binary alloy phase diagrams (reference 13).

The tendencies to combination of some reactive elements with impurities is indicated comparatively by limited thermodynamic data (Table III) and by the melting points of compounds which may be formed. The reactive elements, like the impurities, segregate during solidification of the alloy, and limits to their addition are posed by the threat of formation of eutectics and/or high concentrations of intermetallic compounds at grain boundaries, with concomitant reversion to poor hot workability and weldability. Fig 9 shows some pertinent binary-alloy phase diagrams. In some instances, there may be disposition to eutectic-formation between subversive elements and the reactive addition. On a microscopical scale, there is the possibility of complex interactions and phase relationships, their nature and the volume fraction of additional phases depending also on solidification and cooling rates. An ideal finishing addition would form stable high melting point compounds with the impurities, any excess being soluble in the alloy.

If the concentrations of those impurities participating in the more vigorous reactions are not too high, the small additions of reactive elements potentially can combine also with other subversive elements to give nett beneficial effects. Accordingly, the raw materials used in the production of the alloy must still be of good quality, and the reactive additions must be controlled very carefully.

Neither zirconium nor titanium was found in the CuNi10Fe plates, but zirconium has been used as a finishing addition for cupro-nickels, and titanium usually is present in cupro-nickel weld metals primarily to control weld metal porosity. Thermodynamic data which would show the tendencies of those two elements to react with the more potent impurities are not available. However, there are possible alternative or contributory mechanisms. Improvements in the 'Varestraint' hot ductilities of autogenous weld runs on impurity-doped, calcium-treated, cupro-nickel bars have been reported when carbon is co-present with zirconium or titanium[2], and it was suggested that carbide formation could reduce the effect of low freezing point liquid during solidification. Other hypotheses are that some of the impurity elements are soluble in, adsorbed on, or react with carbonitrides. Some supporting evidence is to be found among other alloy systems. Thus, deleterious elements were detected in association with niobium carbide particles in austenitic D-2 Ni-Resist ductile carbon iron to which niobium is added to improve weldability[14]. Increase of chromium content, leading to greater volume fraction of chromium carbide, enhances the welding response of the D-2 iron. Also, hot-fissuring in fully austenitic stainless-steel weld metals diminishes when the carbon content is sufficient to permit the formation of primary chromium carbide.

It is not possible to define precisely the addition and impurity levels which will eliminate fusion boundary cracking under all welding conditions. Attempts to impose such levels would place unreasonable restrictions on the manufacturers with consequent effects on cost and delivery. As problems in recent years have been very few, the best approach still is to ensure that the material is supplied by reputable producers and that the welding intentions are known to them. Additionally, the findings of the work here reported show that fabricators can contribute by restricting weld heat-inputs which, together with low interpass temperatures, may be necessary to ensure also that the weldments display adequate strength and resistance to erosion/corrosion.

## Acknowledgment

The author is indebted to Nickel Development Institute for encouragement in compiling this paper.

## References

**1** R. K. Wilson, T. J. Kelly and S. D. Kiser, "The effect of iron dilution on Cu-Ni weld deposits used in seawater"; *Weld. J.*, **66**, (1987), Sept., 9, 280s-287s.
**2** M. F. Jordan and A. Duncan, "Cracking in the welding of cupronickel alloys." INCRA Project 329. Final Report, 1985.
**3** C. E. Witherell; "Some factors affecting the weldability of the cupro-nickels." *Weld. J.*, **39**, (1960) 411s-416s.
**4** F. J. Ansuini, Unpublished work at Inco Inc, IRDC, August, 1966 and January, 1967.
**5** M. H. Scott, "The weldability of high strength cupro-nickel;" International Conference. Welding and Fabrication of Non-Ferrous Materials. The Welding Institute. Eastbourne, 1972, May, Paper 20.
**6** J. P. Chubb, J. Billingham, P. Hancock, C. Dimblylow and G. Newcombe, "Effect of alloying and residual elements on strength and hot ductility of cast cupro-nickel", *J. of Metals*, **30**, (1978), March, 3, 20-25.
**7** S. A. Gavin, J. Billingham, J. P. Chubb and P. Hancock, "Effect of trace impurities on hot ductility of as-cast cupro-nickel alloys," *Metals Technology*, (1978), November, 397-401.
**8** D. J. Heath, "Modern power sources score in non-ferrous welding." *Welding & Metal Fabrication*, (1982), October, 374-378.
**9** W. F. Savage, "Solidification, segregation and weld imperfections." 1980 Houdremont Lecture, *Welding in the World*, **18**, (1980), 5/6, 89-144.
**10** J. Barberry, "La Soudabilité des cupro-nickels", *ATB Metallurgie*, **XXV**, 1985, 1, 59-67.
**11** P. J. Berg and R. G. De Lange, "The corrosion behaviour of "Cunifer" 10 alloys in seawater piping systems on board ship — Part II," TNO. Nederlands Scheepsstudiecentrum, Rep. 13417, 1969, November.
**12** Smithells Metals Reference Book. 6th Edition. Butterworth & Co. (Publishers) Limited, 1983.
**13** T. B. Massalski, "Binary alloy phase diagrams." American Society for Metals. 1986.
**14** N. Stephenson, "Improving the weldability of SG Ni-Resist D-2 iron". Conference: Welding of Castings, Welding Institute, Bradford, 21-23 Sept., 1976. Paper 6.

**Members of NiDI**

Companhia Níquel Tocantins
Empresa de Desenvolvimento
de Recursos Minerais "CODEMIN" S.A.
Falconbridge Limited
Impala Platinum Limited
Inco Limited
MEQ Nickel Pty. Ltd.
Morro do Níquel S.A.
Nippon Yakin Kogyo Co., Ltd.
NRNQ (a limited partnership)
Outokumpu Oy
Pacific Metals Co., Ltd.
Sherritt Gordon Mines Limited
Shimura Kako Company, Ltd.
Sumitomo Metal Mining Co., Ltd.
Tokyo Nickel Company Ltd.
Western Mining Corporation Limited

# The Nickel Development Institute is an international nonprofit organization to serve the needs of people interested in nickel.

## NiDI

### North America

Nickel Development Institute
15 Toronto Street - Suite 402
Toronto, Ontario, Canada M5C 2E3
Telephone 416 362 8850
Telex 06 218 565
Fax 416 362 6346

### Europe

Nickel Development Institute
42 Weymouth Street
London, England W1N 3LQ
Telephone 071 493 7999
Telex 51 261 286
Fax 071 493 1555

Nickel Development Institute
European Technical Information Centre
The Holloway, Alvechurch
Birmingham, England B48 7QB
Telephone 0527 584 777
Telex 51 337 125
Fax 0527 585 562

### Japan

Nickel Development Institute
11-3, 5-chome, Shimbashi
Minato-ku, Tokyo, Japan
Telephone 03 436 7953
Telex 72 242 2386
Fax 03 436 7734

### Central & South America

Nickel Development Institute
c/o Instituto de Metais Não Ferrosos
Av. Nove de Julho, 4015, Caixa Postal 6691
São Paulo-SP, Brasil
Telephone 011 887 2033
Telex 38 112 5479
Fax 011 885 8124

### India

Indian Nickel Development Institute
c/o Indian Lead Zinc Information Centre
N° 7 Shopping Centre, Block B-6, Safdarjung Enclave
New Delhi 110 029, India
Telephones 600 973, 604 230
Telex 81 317 2050

### Australasia

Nickel Development Institute
P.O. Box 28
Blackburn, South Vic 3130, Australia
Telephone 61 3 878 7558
Fax 61 3 894 3403